Combined Radial-Axial Magnetic Bearing for a 1 kW, 500,000 rpm Permanent Magnet Machine

P. Imoberdorf, C. Zwyssig, S. D. Round and J.W. Kolar
Power Electronic Systems Laboratory
ETH Zurich
Zurich, 8092 SWITZERLAND
imoberdorf@lem.ee.ethz.ch

***Abstract* – Ultra-high-speed and high-power-density drives are attracting much interest in today's industry. For instance, there are several investigations into mesoscale gas turbine generator systems and turbocompressors for fuel cells. In all ultra-high-speed machinery the bearing is a key technology. Therefore, this paper focuses on the design of a 500,000 rpm active magnetic bearing suitable for use in a 1 kW PM machine to complete an ultra-high-speed electrical drive system. The design procedure selects the suitable magnetic bearing type to keep the system compact and small. The electromagnetic characteristics are determined, the results for the rotor dynamic analysis are presented and the air friction losses caused by the high frequency operation are evaluated. The final design is a combined radial-axial magnetic bearing with a volume of 50 cm^3.**

I. Introduction

Over the last few years, industry has had an increasing need for ultra-high-speed and high-power-density drives, and the trend to more compact and higher speed drives continues. For instance, in the PCB drilling industry the trend is to produce smaller diameter holes and in order to attain the same productivity as today, the drilling machines have to rotate at much higher speeds (more than 300,000 rpm). The trend for turbocompressors is towards smaller power ratings and with the scaling of turbo machinery, therefore require higher speeds [1], [2]. One application is in a fuel cell air compressor that requires 120,000 rpm at 12 kW [3] and another is in a 70,000 rpm, 131 kW turbo compressor connected to a PM machine and inverter [4]. Future automotive fuel cells will require low power compressors, which are small and lightweight, and directly driven by high-speed electrical drives. Ultra-micro gas turbines with power outputs up to several hundred watts are being investigated for use in portable power applications [5]. Fig. 1 presents the various application areas for ultra-high-speed machines and shows the power and speed ranges in which they are concentrated. For a 1 kW system, speeds in excess of 300,000 rpm are classified as ultra-high-speed applications. It is predicted that the speeds will reach close to 1 million rpm in some emerging applications.

A key technology for all ultra-high-speed rotating machinery is the bearing system. In principle, the possible choices for the bearings are high-speed ball bearings, static and dynamic fluid bearings, foil bearings or magnetic bearings. Except for the ball bearings, all other bearing types require a rather complex design process, however, they show a big advantage compared to the ball bearings. These other bearing types rotate in air or another fluid, and therefore have no wear, and are only subjected to air friction. Furthermore, ball bearings are not well suited for operation at high temperatures, which are typical for a gas-turbine generator. With higher rotating speeds, the increased friction losses in the form of heat can change the properties of the lubricant and finally be destructive for the ball bearing. Fluid bearings as well as magnetic bearings minimize this problem. Therefore, even if ball bearings are a possible option, the bearing types with reduced friction losses are preferred. A short summary of the different bearing types is given in Table I. The big advantage of magnetic bearings is their controllability. Active magnetic bearings can cancel or damp instabilities occurring at high speeds [6]. This advantage comes with the cost of an additional power electronics device that controls the bearing forces.

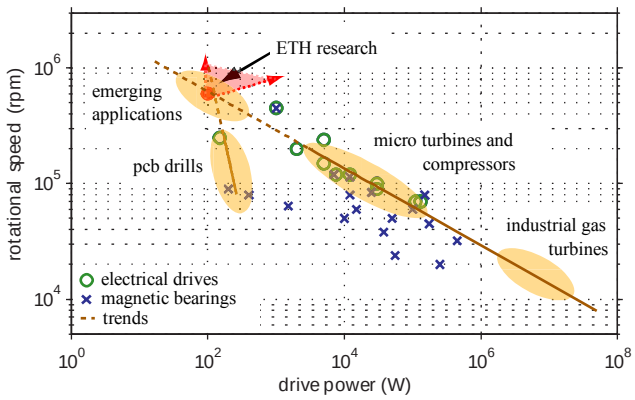

Fig. 1. Application areas for ultra-high-speed drives and magnetic bearings.

This paper presents the design and mechanical construction concept for a combined radial-axial magnetic bearing for ultra-high speeds. The bearing is constructed together with a 1 kW, 500,000 rpm permanent-magnet machine developed at ETH [7]. The machine and the magnetic bearings are integrated into one system and the power and control electronics for both drive and bearing are optimized for ultra-high-speed operation and minimal volume. The motivation for this work is to design an active magnetic bearing for ultra-high-speed applications and as a first step towards the realization of a hybrid bearing that combines the advantages of fluid bearings and magnetic bearings. Using a fluid bearing as main supporting component allows a smaller and less complex magnetic bearing to be used.

TABLE I
COMPARISON OF DIFFERENT BEARING TYPES

	Bearing Type	Pros	Cons
	Magnetic	No wear Lifetime Controllability	Complexity
	Ball	Small size Availability	Losses Noise Wear, Lifetime
Fluid Bearings	**Static**	Exact positioning Lifetime	External pressure system
Fluid Bearings	**Dynamic**	Small size	Instabilities Wear at start/stop
Fluid Bearings	**Foil**	Small size	Wear at start/stop Availability

The magnetic bearing can also take corrective actions if the shaft runs through some induced instabilities. The advantages of hybrid bearings are further discussed in [8] and investigated at various institutions [9].

In Section II, the design of the magnetic bearing, power electronics and mechanical construction is presented. The rotor dynamics and the air friction losses are analyzed in detail in Section III as they limit the performance of the magnetic bearing. Finally, the position sensors and the future work for the combined radial-axial magnetic bearing are discussed.

II. DESIGN OF THE MAGNETIC BEARING

Different design concepts exist among the various magnetic bearing systems available and described in literature. Mainly one can distinguish between two configurations, the heteropolar and the homopolar arrangement of the magnets as depicted in Fig. 2. In the heteropolar configuration the magnetic flux density, at a point on the rotating shaft, reaches values between $+B_0$ and $-B_0$ during a cycle, whereas the induction in the homopolar bearing is always between 0 and $+B_0$. Therefore, the iron losses of the homopolar bearing will be smaller than those of the heteropolar bearing, especially for higher speeds. This is the reason why the homopolar bearing is preferred. Another possibility of reducing the iron losses is to design the pole shoes such that they enclose the whole shaft [10].

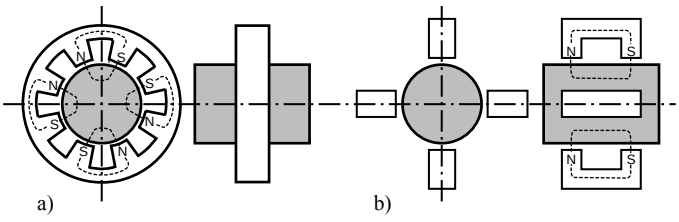

Fig. 2. Concepts of radial bearings: (a) heteropolar and (b) homopolar configuration of the magnets (end and side views).

To reduce the size of the bearing unit a permanent magnet is used as the source of the bias flux. In such a configuration, only the control flux has to be created by a control current, which leads to a more compact design. The size difference between a magnetic circuit implemented with an energizing coil and a permanent magnet is illustrated in Fig. 3 (a), where the same magnetic flux density is created in the air gap for both possibilities. However, the permanent magnet has a high reluctance and with a proper design of the magnetic circuit, the additional air gap created by the permanent magnet, does not need to have an influence on the control flux paths and therefore does not require the use of larger control coils. Fig. 3 (b) shows the influence of biasing the magnetic bearing. Due to the quadratic relation between the carrying force and the magnetic flux density, the same small control current can be used to produce more force after biasing with a permanent magnet ($\Delta F_1 << \Delta F_2$).

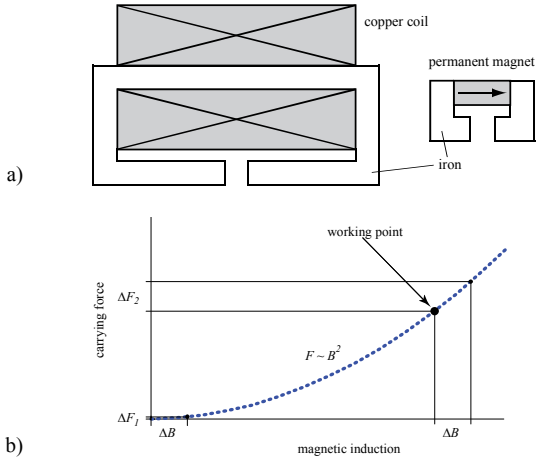

Fig. 3. (a) Comparison of a copper coil and a permanent magnet circuit creating the same magnetic flux density in the air gap. (b) Effect of a permanent magnet as bias flux on the dynamics of the carrying force.

A. Concept of the proposed magnetic bearing

Most of the active magnetic bearing systems have two separate bearings for the axial and the radial direction. This is the easiest way to produce a magnetic bearing but it also requires more space for the two separate devices. In order to reduce the overall size of the bearing system, which is an important consideration in low volume ultra-high speed machines, the combination of the radial and axial bearing is one possibility. One solution for a highly integrated bearing is presented in [10]. There the rotor endings have a conical shape, which allows the forces to be applied in the axial as well as in the radial direction. The disadvantage of such a system is the cross coupling of the different axes, which requires a more complex controller.

Another concept, depicted in Fig. 4 and Fig. 5, combines the two bearings by using a radially magnetized permanent magnet ring as source of the bias flux for both the radial and the axial bearing [11] and [12]. As can be seen the magnet ring is not part of the control flux paths and therefore small control coils can be used since they do not have to compensate for the high reluctance of the permanent magnet ring. The bias flux created by the permanent magnet ring alone does not provide any force. It has to be superimposed by a control flux for both the radial and the axial bearing force. In Fig. 4, both the radial and the axial control flux paths are depicted.

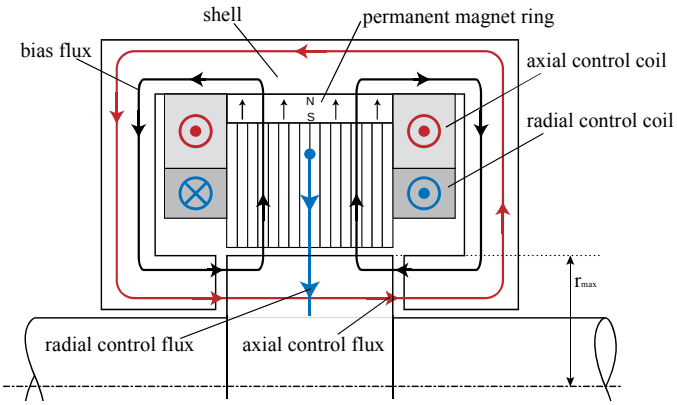

Fig. 4. Axial cut view through the combined radial and axial magnetic bearing device including the magnetic flux paths.

In one axial air gap, the bias flux and the control flux adds together whereas in the second axial air gap they subtract. The resulting difference of magnetic flux density in the two opposing air gaps creates the carrying force and can be controlled by the sign and amplitude of the control current in the axial control coils. These coils lie in the shell and are concentric to the PM ring. The same is valid for the radial force, which can be verified by looking at the radial control flux in Fig. 5 where again the bias flux and control flux add or subtract in two opposing air gaps.

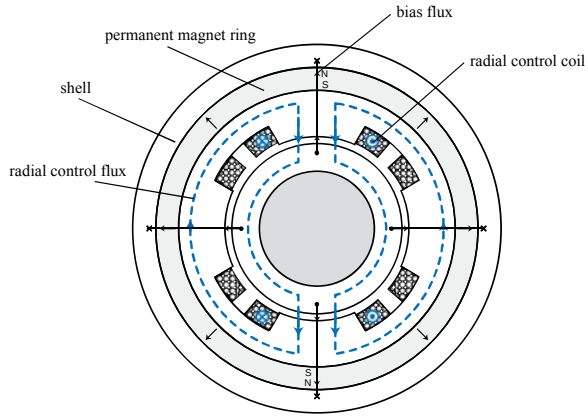

Fig. 5. Radial cut through the magnetic bearing device.

B. Electromagnetic Design

To drive the shaft, a system similar to that described in [13] is used. The maximum rotor diameter is set to 12 mm and the maximum rotational speed is 500,000 rpm. The rotor, consisting of a permanent magnet for the PM machine, titanium and two iron parts of bearing as a total weight of approximately 35 g. Considering that the magnetic force has to compensate not only for the rotor weight, but also for any additional unbalance, the bearing is designed for three times its weight (3g criteria [11]). This results in a desired carrying force of 1.15 N. The permanent magnet ring has an outer diameter of 38 mm and a thickness of 3 mm. The magneto motive force of 835 A-turns created by the PM ring results in magnetic flux densities of 1.03 T and 0.71 T in the axial and radial air gaps respectively.

With 54 turns in the axial coil of one bearing unit and a maximum current of 1.5 A, a maximum axial force of 6.3 N is achieved. Each radial pole shoe has a winding containing 25 turns. A force of 8.2 N can be created assuming a maximum radial control current of 2 A. The rotor at rated speed has a rotational frequency of 8.3 kHz, and therefore the force should be able to be changed from $-F_{max}$ to $+F_{max}$ at a faster rate in order to be able to react to speed induced disturbances. To enable the force to change its sign every 50µs, which is equivalent to a signal bandwidth of 20 kHz, the power electronics coil driver must be supplied with at least 15 V. That voltage is necessary to impress full current and to change its sign with the inductances given in Table II. The copper losses are calculated by taking into account the skin effect caused by the high frequency operation. The loss calculations are performed for the worst case operation i.e. full speed of 500,000 rpm, full current of 2 A and a switching frequency ten times the rate at which the force can change its sign. The losses for the two bearing units total 9.1 W when delivering the maximum axial and radial forces. All the design calculations are undertaken assuming an ambient temperature of 25°C and bearing parameters are summarized in Table II. These values require modification if the ambient temperature inside the machine rises due to heating from the losses, which cannot be adequately removed from the system. An alternative is to operate the system in a vacuum in order to eliminate the air friction losses.

TABLE II
ACTIVE MAGNETIC BEARING DATA

Geometry	
rotor length	96 mm
maximum rotor diameter (r_{max})	12 mm
rotor weight	35 g
bearing outer diameter	45 mm
radial and axial air-gap δ	250 µm
radial pole shoe area $A_{\delta r}$	38 mm^2
axial air gap area $A_{\delta a}$	94 mm^2
Coil parameters	
inductance of axial winding	125 µH
inductance of radial winding (two poles in series)	190 µH
wire diameter	0.45 mm
Electrical data	
minimum supply voltage	15 V
maximum axial control current	1.5 A
maximum radial control current	2 A
switching frequency	200 kHz
Losses	
copper	9.1 W
air friction (per unit)	30 W
Bearing forces	
axial	6.3 N
radial per unit	8.2 N

C. Bearing force

The bearing force in one air-gap is deduced from the stored magnetic energy in the air-gap. Applying this to the case where there are two opposite forces and the magnetic field is created by a bias flux combined with a control flux results in a force of

$$F = \frac{2A_\delta}{\mu_0} \cdot B_0 B_c \tag{1}$$

for the two opposed pole shoes. The bias and the control magnetic flux densities in the air-gap have to be calculated through an equivalent magnetic circuit of the bearing system. Considering the curvature of the active pole shoe area A_δ, the force is corrected by a factor that is dependent on the angle α in radians.

$$\frac{F_{real}}{F_{ideal}} = \frac{2}{\alpha} \cdot \sin\frac{\alpha}{2} = f(\alpha) \tag{2}$$

D. Bearing Parameters k_i and k_x

For small deflections x of the shaft position the bearing force can be linearized as

$$F = k_i \cdot i_c + k_x \cdot x \tag{3}$$

where k_i is the force-current factor and k_x the force-displacement factor. k_x is also called negative stiffness of the magnetic bearing since without control current the force acts as a negative spring force and thus is unstable. The calculation of the force-current factor is a simple derivation of the carrying force by the control current i_c.

$$k_i = \frac{\partial F}{\partial i_c} \tag{4}$$

For the computation of the force-displacement factor, only the permanent magnet circuit is considered [14]. A deflection of the rotor from its zero position results in a change of the equivalent air-gap reluctances. This leads to different magnetic flux densities in two opposed air-gaps and thus results in a force that tends to close the smaller air-gap. In Fig. 6, an equivalent network representation is shown where the "+" in the reluctance subscript designates the larger air-gap and the "-" the smaller air-gap, respectively. With the equivalent networks, the bias flux densities in two opposing air-gaps are calculated. Knowing this allows the calculation the resulting force, which can be differentiate with respect to the deflection x and results in

$$k_{xr} = -\frac{\phi_{PM}^2}{8\mu_0 A_{\delta r}\delta_r}, \qquad k_{xa} = -\frac{\phi_{PM}^2}{2\mu_0 A_{\delta a}\delta_a} \tag{5}$$

for the radial and the axial bearing respectively. The bearing parameters for the described magnetic bearing are listed in Table III.

TABLE III
BEARING PARAMETERS DESCRIBING THE CARRYING FORCE

	Radial bearing	**Axial bearing**
Force-current factor – k_i	4.1 *N/A*	4.2 *N/A*
Force-displacement factor – k_x	-122 *kN/m*	-195 *kN/m*

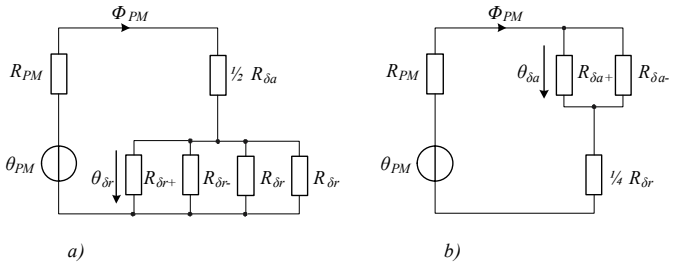

Fig. 6. Equivalent magnetic circuit for the permanent magnet flux for a rotor deviation in (a) radial direction and (b) along the axial direction. The subscripts δ_a and δ_r refer to the axial and radial air gap respectively.

E. Power electronics

Each coil for the magnetic bearing is energized by controlling the magnitude of the current flowing through it. For normal operation, the current is in the range of approximately ±2 A. An H-bridge power electronics circuit, as shown in Fig. 7, is used to energize the coil and allows either a positive or negative energizing current. A relative low dc voltage of less than 50 V is needed to produce the coil current and this voltage level enables small sized 60 V IR6648 DirectFETs to be used as the power switches. Since the magnetic bearings are used in a compact machine, it is desirable that the power and control electronics also occupy a small volume. This is especially important as this application requires five controllable magnetic coils. For each bearing there is an x- and y-axis control coil and for the two bearings there is a z-position control coil. The required bandwidth of the controller is in the order of twice the maximum rotational speed and therefore is chosen as 20 kHz. Consequently the switching frequency of the H-bridge needs to be in the hundreds of kHz. In this application, a switching frequency of 200 kHz is selected. A boot-strap isolated bridge gate driver is connected to each half-bridge leg and the switching signals are directly produced by a custom TMS320F2808 DSP control board that is the size of a credit card. The DSP samples the coil current, which is measured by a shunt resistors in series with the bottom MOSFETs, at a frequency that is the same as the switching frequency. The current reference is determined from the position controller that is also implemented inside the DSP. The control and power board measures 135 mm by 54 mm.

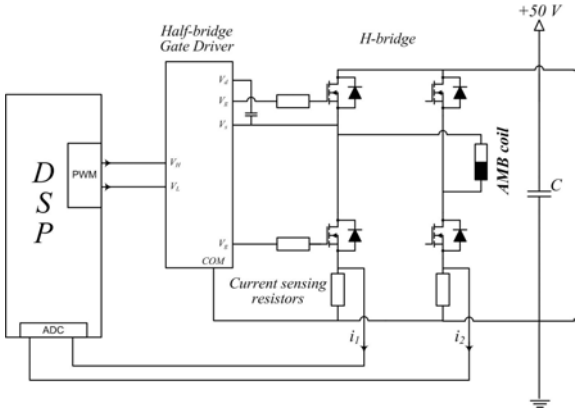

Fig. 7. H-bridge coil driver for one axis of the AMB.

F. Mechanical Construction Concept

To test the combined radial-axial magnetic bearing, a test bench has been designed. It allows the verification of the theoretical considerations and the system design. The rotor is driven by a 1 kW permanent magnet synchronous machine and a bearing unit is placed at each end of the rotor. The overall size of the system is a maximum diameter of 55 mm and a rotor length of 96 mm. All the different components are mounted on an aluminum flange to guarantee concentric alignment. The system consisting of the flange, the permanent magnet drive and the two bearing units is depicted in Fig. 8.

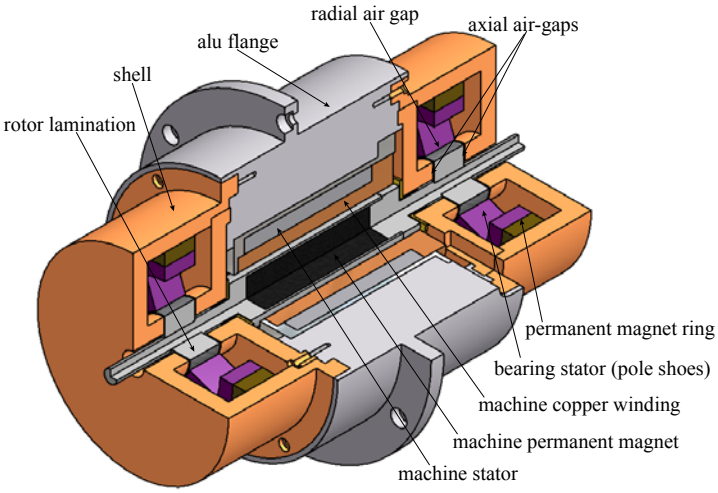

Fig. 8. Cut away view of the 1 kW, 500,000 rpm system. Electrical drive and two bearing units mounted on an aluminum flange.

Permanent Magnet Ring

The permanent magnet ring, which provides the bias flux, is realized by a rare earth magnet material to keep the thickness of the ring small. Two possible choices for the radially magnetized ring are NdFeB or SmCo permanent magnets. A Sm_2Co_{17} based magnet is chosen because its thermal properties allow operating temperatures up to 350°C.

Retainer bearing

Magnetic bearing systems also require retainer (backup) bearings. When the magnetic bearing is inactive, the retainer bearing should support the rotor, keep the rotor away from the bearing stators and reduce the possibility of damage. In case of failure of the AMB system, the retainer bearings also allow a safe machine shut down. During load transients, the retainer bearings provide a temporary means of rotor support while the magnetic bearing reacts. The requirements for these bearings can be extremely challenging, especially for high speed rotating machines. When the shaft falls into the retainer bearings, a sliding contact takes place and back whirl motions can occur [15]. The correct choice of the material for the retainer bearings, which should keep the rotor within bounds in case the magnetic suspension fails, is an important aspect. A good compromise between a soft, energy-absorbing material and one which will maintain its shape must be found. A material that promises these properties is *ERTACETAL,* which is a Polyoxymethylene (POM). This material shows a high resistance against wear, has a friction coefficient of about 0.2 and can endure temperatures up to 140°C. In Fig. 9 the retainer bearing in our system can be seen. It acts as a back-up bearing for both radial and axial disturbances.

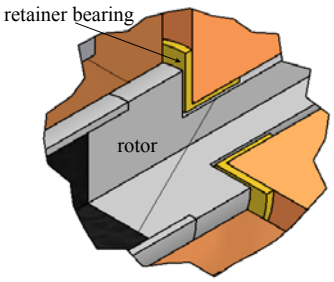

Fig. 9. Detailed view on the retainer bearings, which protects for both axial and radial disturbances.

III. Rotor Dynamics and Air Friction Losses

For the machine to work properly it is important to know the systems mechanical properties. A rotor spinning at ultra-high speeds will encounter different critical bending modes while accelerating. The characteristics of these bending modes influence the positioning of the sensor and are an important aspect in the design of the magnetic bearing control system.

A. Rotor dynamics

To characterize these bending modes requires knowledge of the frequency at which they appear and to be able to visualize the deformation at these points. Such an analysis has been performed by finite element simulation of the rotor. A simple rotor without any impeller or other load has been simulated. This is a first simulation, keeping in mind that any mechanical load on the rotor influences its characteristics and therefore has to be analyzed specifically for each application. The stiffness of the bearing system is taken into account, which shifts the bending modes to lower frequencies. The stiffness of the bearing can be adjusted by the design of the controller. Normally the desired stiffness is chosen in the range of the calculated force-displacement factor. In the finite element simulation, the value of the radial k_x shown in Table III is taken as the bearing stiffness. The rotor dimensions are chosen such that there is no critical bending mode at rated speed (500,000 rpm, 8.33 kHz), which is verified in Table IV and depicted in Fig. 10.

TABLE IV
Bending Modes of the Rotor

	Frequency
First bending mode	385 Hz
Second bending mode	576 Hz
Third bending mode	2638 Hz
Fourth bending mode	4682 Hz
Fifth bending mode (higher than rated speed)	11891 Hz

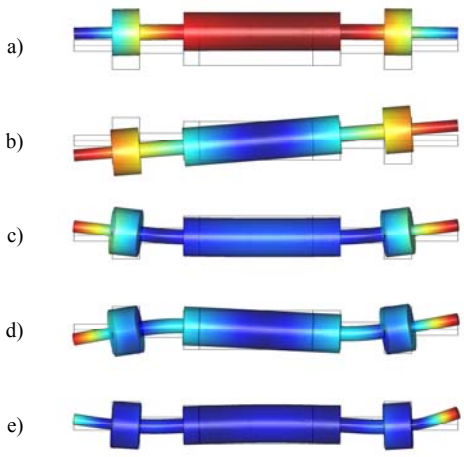

Fig. 10. Bending modes of the rotor. First (a), second (b), third (c), fourth (d) and fifth (e).

From Fig. 10 it can be seen that two position sensors placed at either end of the rotor can detect the deformation of the bending modes and therefore magnetic bearing is capable to damp the oscillations. The bending modes shown in Fig. 10 (a) to (c) can be changed by changing the bearing stiffness in the controller. This allows the rotor to bypass operation at the critical frequencies. A problem occurs for the fourth bending mode where the carrying force of the magnetic bearing acts on a nodal point, and this cannot be compensated for. This bending mode problem identifies one of the challenges of high speed operation and will be investigated experimentally to determine if any control is possible.

B. Air friction losses

In electrical machines the drag of the enclosed fluid, which for most applications is air, results in a considerable source of power losses. This is especially the case for high rotational speeds since the air friction losses correlate with the circumferential speed. A calculation of the air friction losses according [16] is performed using simplifying assumptions. All the major parts of the rotor, the drive and the two bearing units are modeled as either full or hollow cylinders. For a rotational speed of 500,000 rpm this results in about 60 W losses in the air gap of the machine and additional 30 watts from each of the magnetic bearing units.

A simplified model of the shaft, the electric drive system and the two bearing units is used to simulate the thermal impact due to the air friction losses. The simulations show that pressurized air is needed to remove the heat produced by the losses. An ambient temperature of 45°C is assumed. Further, an airflow rate of 0.5 dm^3/s is supplied separately to each of the two bearing units and the drive. Cooling the electric drive and bearing with such an airflow can maintain the temperature at a maximum of 100°C as depicted in Fig. 11.

IV. Position Sensors

Eddy current sensors are widely used in active magnetic bearing systems to determine the position of the levitated rotor. Conventional eddy current sensors are placed around the rotor, generate a magnetic field, which is directed towards the rotating shaft, and allows the measurement of the damping factor of a resonant circuit as the shaft changes its radial position. In [17] and [18] a novel type of radial sensor is presented where the sensor coils are integrated on a printed circuit board (PCB). A new aspect in that sensor is the differentiation of an excitation and several sensing coils. Fig. 12 illustrates a sensor PCB that is adapted to our system requirements.

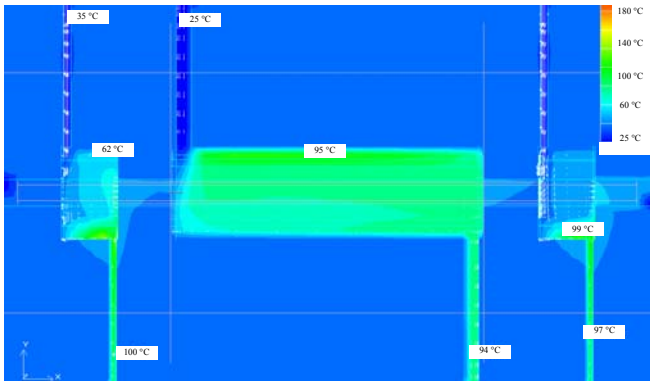

Fig. 11. Temperature distribution due to air friction losses in a simplified model of the electric drive and two bearing units. The air in the system is cooled by pressurized air.

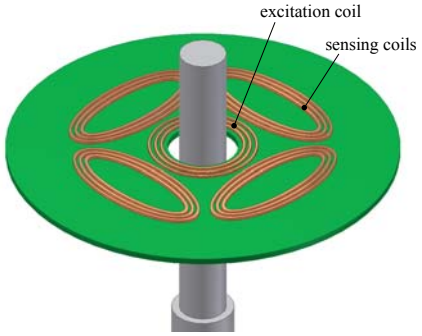

Fig. 12. Sensor PCB capable of measuring the radial displacement of the rotor.

The excitation coil, which is concentric to the shaft, generates a magnetic field that is rejected by eddy currents within the electrically conductive rotor material. This leads to a field concentration between the rotor and the excitation coil. Therefore, a small change of the rotor position has a large impact on the field distribution. On one side, the field is weakened, while the magnetic field on the opposite side of the shaft gets stronger. The difference in field strength is detected by the sensing coils, which are placed around the excitation coil. This ultra-compact (thin) radial sensor is very simple to implement since it only requires a PCB and no other components. Despite its simplicity the sensor has a high sensitivity to changes in the rotor position.

To measure the axial position of the rotor, conventional eddy current sensors are placed at both ends of the rotor.

V. Future Work

The combined radial-axial magnetic bearing concept is currently being experimentally verified in the 1 kW 500,000 rpm PM machine. The experimental performance will be reported in the near future. This will include a description of the control implementation for the bearing. By using a DSP, advanced control techniques such as adaptive vibration control can be investigated.

As shown by the thermal analysis, the extraction of the heat produced from the air friction and machine losses is difficult to achieve when there are very small clearances used in the magnetic bearings. Initially, this concept will be used for a machine that is operated in a vacuum such that only the machine losses have to be removed. However, further investigations will be undertaken to determine the optimal dimensions for the magnetic bearing and the electrical machine in order to effectively remove the losses, through forced air cooling.

The active magnetic bearing is the first part of a research program that is investigating the concept of hybrid bearings that contain either an air or foil bearing and an active magnetic bearing. The air or foil bearing provides the main support of the rotor while the magnetic bearing provides active stabilization.

VI. Summary

For machines that operate at ultra-high speeds the use of bearings based on ball races is no longer suitable due to their high losses and limited lifetime. An active magnetic bearing is an alternative bearing topology, which is suitable for ultra-high speed operation. Due to the compact size of the electrical machine at these ultra-high speeds, it is important to minimize the volume of the magnetic bearing. In this paper, an active magnetic bearing that has the radial and axial forces combined into a single bearing unit is presented. The design of the bearing and the mechanical construction concept is explained. The physical dimensions of the bearing are 45 mm by 22 mm and the diameter is larger than that of the electrical machine. The control of the magnetic bearing coils is implemented using a DSP and a low voltage MOSFET H-bridge, switching at 200 kHz, is used to generate the current in each of the five coils. Initially the active magnetic bearing design will be tested on a 1 kW, 500,000 rpm electrical machine operating in a vacuum.

The critical and challenging research topics for active magnetic bearings are the design and the position control of the rotor to ensure the bending mode nodal points do not fall in the position of the magnetic bearings or sensors, and that the physical design must be optimized to ensure that the air friction losses are minimized.

Acknowledgement

We would like acknowledge the useful discussions and assistance provided by Mr Philipp Bühler of MECOS Traxler AG, Winterthur, Switzerland.

References

[1] M. A. Rahman, A. Chiba, and T. Fukao, "Super high speed electrical machines – summary," IEEE Power Engineering Society General Meeting, June 6-10, 2004, vol. 2, pp. 1272 – 1275.

[2] J. Oyama, T. Higuchi, T. Abe, K. Shigematm X. Yang, E. Matsuo, "A trial production of small size ultra-high speed drive system," IEMDC2003, vol. 1, no.2-1-1, pp. 31 – 36, 2003.

[3] MiTi Developments (November 2005). "Oil-free, motorized, automotive fuel cell air compressor/expander system," Available: http://www.miti.cc

[4] B. H. Bae, S. K. Sul, J. H. Kwon, and J. S. Byeon, "Implementation of sensorless vector control for super-highspeed PMSM of turbo-compressor," IEEE Trans. on Industry Applications, vol. 39, no. 3, pp. 811 – 818, May-Jun. 2003.

[5] S. A. Jacobson and A. H. Epstein, "An informal survey of power MEMS," ISMME2003, Tsuchiura, Japan, December 1 – 3, 2003,pp. 513 – 520.

[6] M. E. F. Kasarda, H. Mendoza, R. G. Kirk, A. Wicks, "Reduction of Subsynchronous Vibrations in a Single-Disk Rotor using an Active Magnetic Damper," Mechanics Research Communications, vol.31, pp. 689 – 695, 2004.

[7] C. Zwyssig, M. Duerr, S. D. Round and J. W. Kolar, "An Ultra-High-Speed, 500,000 rpm, 1 kW Electrical Drive System," 4th Power Conversion Conference 2007, Nagoya, Japan, April 2-5, 2007, to be published.

[8] H. Heshmat, H. Ming Chen, J. F. Walton, „On the Performance of Hybrid Foil-Magnetic Bearings," Journal of Engineering for Gas Turbines and Power, January 2000, vol. 122, pp.73 – 81.

[9] Mohawk Innovative Technology, Inc., "Hybrid Foil Magnetic Bearing Tested," MiTi Developments, vol. 2, 1998.

[10] P. Bühler, "Hochintegrierte Magnetlager Systeme," Diss. ETH Nr. 11287, ETH Zürich, Switzerland 1995.

[11] M. A. Pichot, "Design and Electrodynamic Analysis of Active Magnetic Bearing Actuators," Ph.D. dissertation, University of Texas at Austin, USA, 2003.

[12] P. T. McMullen, S. Huynh, „Magnetic Bearing Providing Radial and Axial Load Support for a Shaft," U.S. Patent 5,514,924, May 7, 1996.

[13] C. Zwyssig, J. W. Kolar, W. Thaler, M. Vohrer, "Design of a 100 W, 500000 rpm Permanent-Magnet Generator for Mesoscale Gas Turbines," IEEE Industry Applications Conference 2005, Conference Record of the 40th IAS Annual Meeting, Hong Kong, October 2-6, 2005, vol. 1, pp. 253 – 260.

[14] F. Betschon, "Design Principles of Integrated Magnetic Bearings," Diss. ETH Nr. 13643, ETH Zürich, Switzerland 2000.

[15] M. Helfert, M. Ernst, R. Nordmann and B. Aeschlimann, „High-Speed Video Analysis of Rotor-Retainer-Bearing-Contacts Due to Failure of Active Magnetic Bearings," 10th International Symposium on Magnetic Bearings, Martigny, Switzerland, August 2006.

[16] M. Mack, "Luftreibungsverluste bei elektrischen Maschinen kleiner Baugrösse," Ph.D. dissertation, Universität Stuttgart, Germany, 1967.

[17] R. Larsonneur, P. Bühler, "New Radial Sensor for Active Magnetic Bearings," 9th International Symposium on Magnetic Bearings, Lexington, Kentucky, USA, August 3-6, 2004.

[18] P. Bühler, "Device for Contact-Less Measurement of Distances in Multiple Directions," European Patent No. EP 1 422 492, June 10, 2004.